LASER INTERFEROMETER GRAVITATIONAL WAVE OBSERVATORY
-LIGO-
CALIFORNIA INSTITUTE OF TECHNOLOGY
MASSACHUSETTS INSTITUTE OF TECHNOLOGY

Technical Note LIGO-T050163-00-R 2005/09/21

SURF Final Report: INITIAL RESULTS FROM THE MESA BEAM CAVITY

John Miller
University of Glasgow, U.K.

Mentor: Riccardo DeSalvo

Distribution of this draft:
LIGO Scientific Collaboration

California Institute of Technology
LIGO Project – MS 18-34
Pasadena CA 91125
Phone (626) 395-2129
Fax (626) 304-9834
E-mail: info@ligo.caltech.edu

Massachusetts Institute of Technology
LIGO Project – NW17-161
Cambridge, MA 01239
Phone (617) 253-4824
Fax (617) 253-7014
E-mail: info@ligo.mit.edu

SURF Final Report: Initial results from the mesa beam cavity

LIGO-T050163-00-R

J Miller

Department of Physics and Astronomy, University of Glasgow, Glasgow G12 8QQ, Scotland, United Kingdom[1]

0203592m@student.gla.ac.uk

Mentor: Dr. R DeSalvo

Abstract

Fundamental thermal noise forms a significant portion of the noise budget of future interferometric gravitational wave detectors and is likely to be the principal limiting factor for Advanced LIGO. Non-Gaussian beams have been proposed to depress this noise without being significantly more difficult to control. In particular, attention is focused on one flat-topped beam, known as the mesa beam, and the non-spherical mirrors which support this field. An experimental Fabry-Perot cavity has been constructed to generate and characterise this new beam, comparing its behaviour to well-understood theory. Preliminary results from this apparatus are presented and indications of further work are given.

Introduction

Motivation

In the region of maximum sensitivity future gravitational wave (GW) detectors will be limited by fundamental thermal noise, see figure 1. If we consider gaussian beams and infinite mirrors, the spectral densities of different types of thermal noise scale with *w* (the beam radius) as follows [1]:

[1] Work carried out at the LIGO Laboratory, California Institute of Technology, Pasadena, CA 91125, USA

$$S_h^{TEs} \propto \frac{1}{w^3} (1)$$

$$S_h^{TEc} \propto \frac{1}{w^2} (2)$$

$$S_h^{Bs} \propto \frac{1}{w} (3)$$

$$S_h^{Bc} \propto \frac{1}{w^2} (4)$$

where *TE*, *B*, *c* and *s* denote thermoelastic, Brownian, coating and substrate respectively.

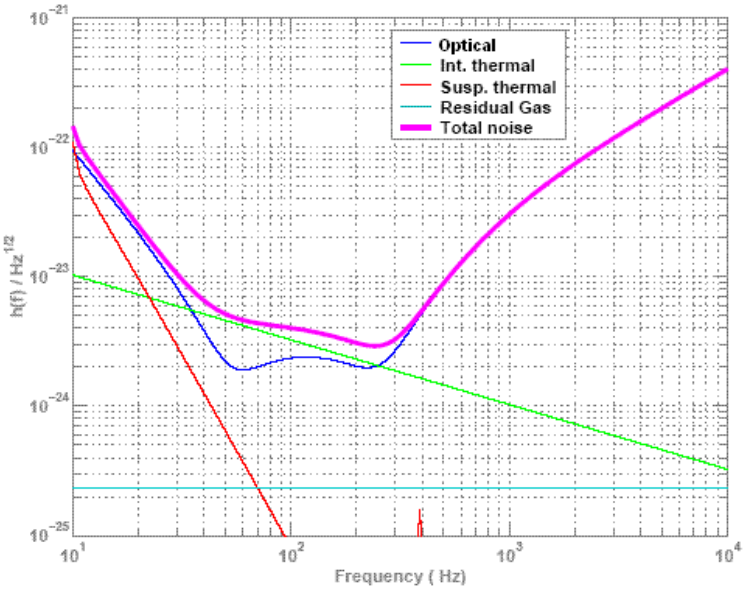

Figure 1 . Detectors are limited by thermal noise [11]. Introducing mesa beams will yield immediate improvements with further benefits available once optical sensitivity (γ quant.) improves

From these relationships it is obvious that a larger beam will reduce thermal noise and increase the volume of the detectable Universe. However it is not possible to simply increase the size of a gaussian beam as diffraction losses become prohibitive. In the clipping approximation the losses scale as shown in (5) where *m* is the mirror radius, *r* is the mirror's reflectivity and *w* is the beam spot size.

$$\ell = \int_m^\infty \frac{2}{\pi w} \exp\left[-2\frac{r^2}{w^2}\right] 2r\pi dr = \exp\left[-2\frac{m^2}{w^2}\right] (5)$$

Additionally, Gaussian beams suffer from the problem that, weighted by intensity and limited by diffraction losses, they sample only a small portion (a few hundredths) of the mirror's surface. This effect is important when considering the average of surface fluctuations caused, for example, by thermoelastic noise. The output phase shift of GW detectors is proportional to the positions of the test masses' surfaces and not to their centres of mass, hence this effect is non-negligible.

We can therefore conclude that a large radius, flat-topped beam will reduce thermal noise.

Mesa Beam

Confronted with this problem one might consider a rectangular beam profile. It is clear that diffraction will also impact our ability to produce a beam with such a profile.

Consider now the mesa field, (6), which may be thought of as a superposition of minimal Gaussians uniformly distributed over a circle, see figure 2. Diffraction losses dictate the width of the minimal Gaussian that may be used to build this beam, impeding the construction of a sharp rectangle and determining the final beam profile [3, 4].

$$U(D,r) = \int_{C_D} \exp\left[\frac{-[(x-x_0)^2 + (y-y_0)^2][1+i]}{2b}\right] dx_0 dy_0 \quad (6)$$

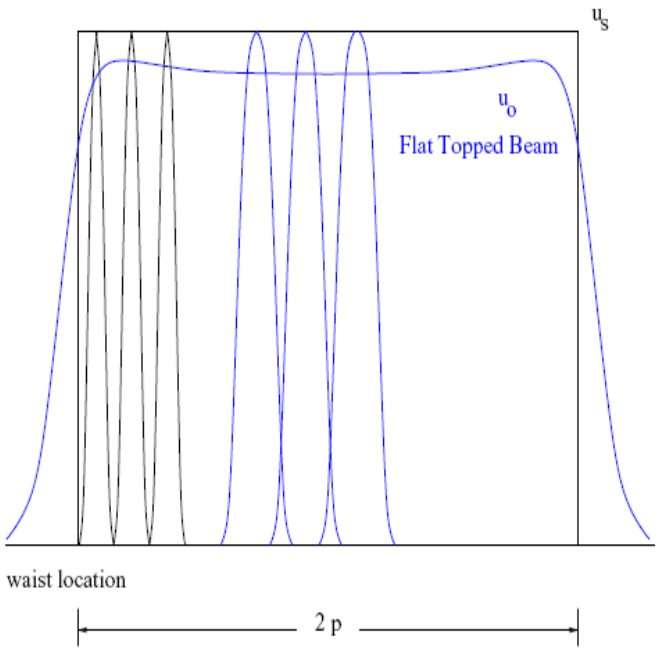

Figure 2. Comparison of rectangular and mesa beam profiles [2]

It is clear that this new beam will no longer have spherical wavefronts as for a Gaussian beam. It has been found that the optimal mirror profile has a steep rim and a central bump resembling a sombrero - hence the Mexican hat moniker. Figure 3 shows a comparison between Gaussian and Mesa beam profiles, normalised for the

same diffraction losses and integrated beam power. The right hand plot shows the mirrors which support each beam.

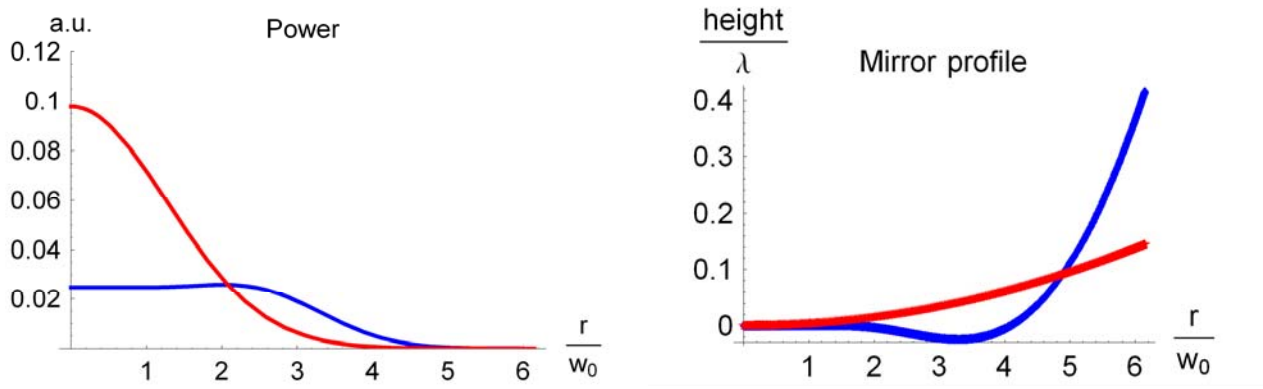

Figure 3. Comparison of Gaussian (red) and mesa beam (blue) fields and mirrors

Apparatus

Mirrors

These unusual mirrors are constructed using a novel two-stage deposition technique by the Laboratoire des Matériaux Avancés in Lyon. This process is detailed in [5, 6]. The final mirror has a peak to valley accuracy of >10nm.

Cavity

A Fabry-Perot cavity has been designed and constructed at the LIGO Laboratory at Caltech to generate and characterise this new beam. The main features of the cavity are as follows (see also figure 4):

- 7.32m folded cavity
- Rigid structure formed by 3 low expansion INVAR rods
- Structure is suspended by 4 pairs of GAS tuned to 0.4Hz (with lower frequencies possible)
- Cavity is housed within a custom vacuum tank
- Mirrors reside in quasi-monolithic mounts. Alignment control is applied via a triplet of micrometric screws and PZTs on each mirror

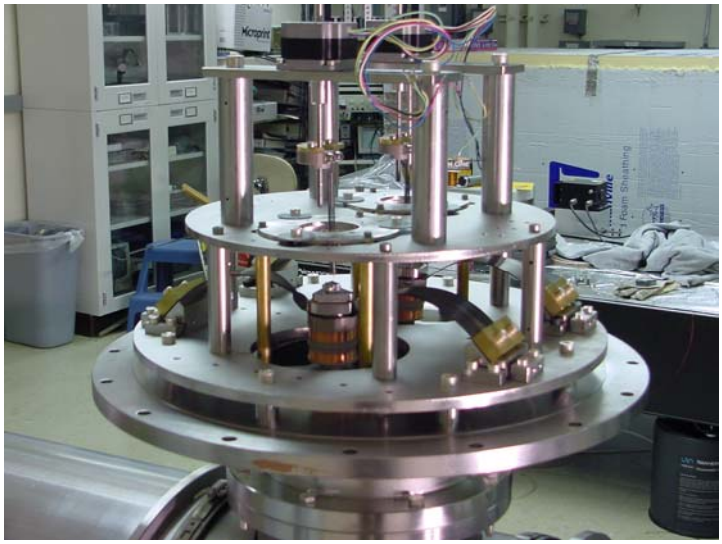

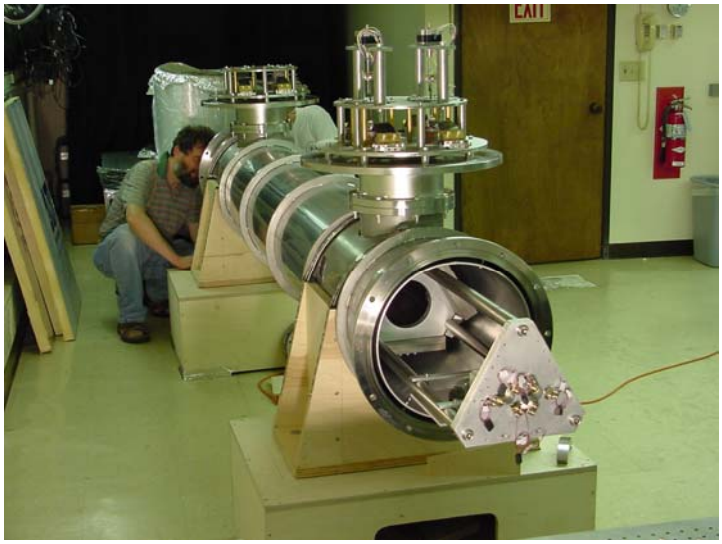

Figure 4. GAS seismic isolation,the cavity during construction

This cavity is also able to support spherical end mirrors. Preliminary tests were conducted with such optics. For further reading see [5, 6, 12].

Experimental Techniques

Optical Set-up

In its final orientation the optical layout was as follows in figure 5. All future references to optics refer to this diagram e.g. EM, IM etc.

Our laser is a 800mW Nd:YAG Mefisto item operating at 1024nm. We are able to implement two locking schemes. Side-locking the cavity by modulating the laser frequncy and peak-locking by dithering the cavity length using the 3 PZTs on any given mirror (in practice IM was consistently used). For complementary reading see [12].

Aligning the cavity

Once a good input beam was achieved it was key to well align it to the cavity. Figure 6 shows a simulation of the effect on a perfect TEM_{00} beam of a 4μrad tilt, alignment is clearly critical.

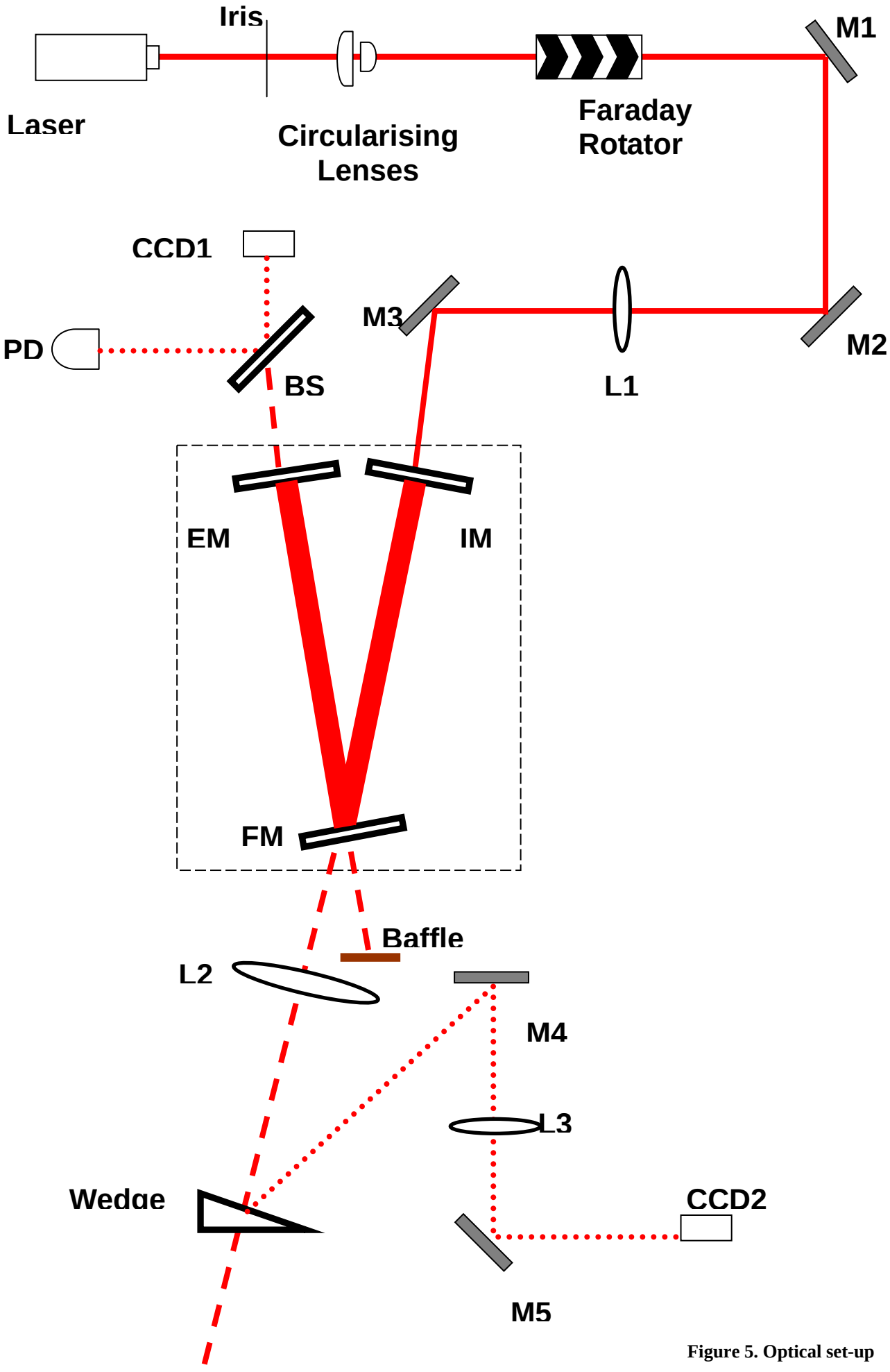

Figure 5. Optical set-up

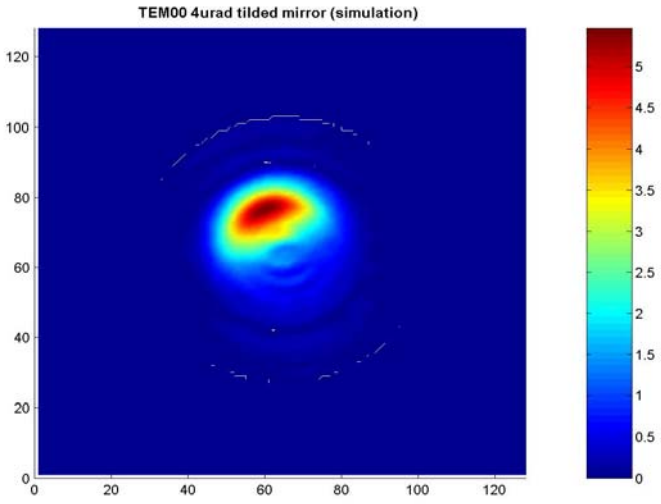

Figure 6. A tilt of the Mexican hat mirror deforms the fundamental mode

Initial alignment followed a simple routine:

- M1,M2 and M3 of figure 5 were used to align the input beam to the centres of IM and FM
- The micrometric screws of FM aligned the beam spot to the centre of the EM
- The screws of EM then aligned the beam to the centre of IM
- The IM is then aligned to bring all three beams into coincidence
- Fine adjustments of the PZTs were made using the CCD on the input bench as a reference whilst sweeping the laser frequency

Once this stage was reached the cavity was locked. The PZTs of each mirror were then adjusted to force the cavity to oscillate in the transverse mode of our choosing.

Frequency analysis

A brief investigation was made into possible noise sources in the experiment. The main tool at our disposal to accomplish this goal was frequency analysis of the photodiode signal when in lock. The signal was acquired using a *LabView* program designed by the author (following the loss of a PC in the lab). Using this program it was possible to view the signal in real time, capture it and perform a frequency analysis. It also permitted us to study the transverse mode spectrum in real time, this was one of the principal factors which lead us to produce the fundamental cavity mode. Figure 7 shows two spectra of the photodiode signal when in lock.

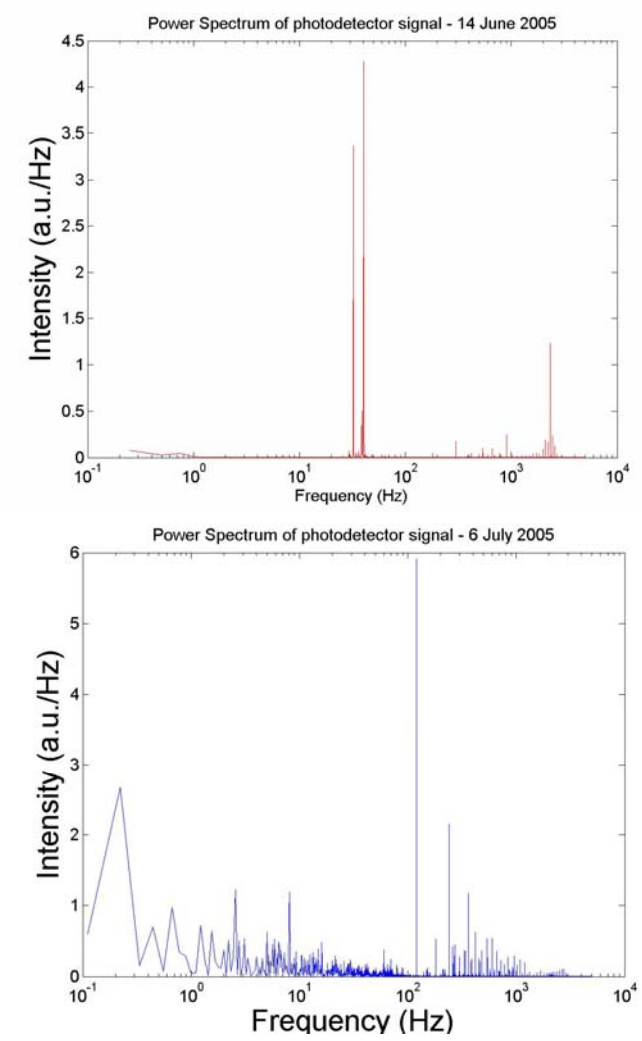

Figure 7. Frequency analysis of the photodiode signal when using both side lock (top) and dither lock (top)

The leftmost picture shows a spectrum taken during a period of side lock. The two large peaks at 32.25Hz and 40.25Hz were observed in many spectra and are believed to be due to mechanical resonances of the complex cavity structure. Perhaps more interesting is the peak at 2340Hz. This peak results from oscillations at the servo pole frequency. This problem is caused by the large frequency response of the laser to small error signal inputs.

The second plot shows analogous data taken during dither lock. The main resonances are at 120Hz and the harmonics thereof. It is believed that these peaks are due to the electronic circuitry used to dither lock the cavity. These peaks are absent from the side lock spectra, hence a logical source candidate is the lock-in amplifier. One may also note the lack of the peaks touted as mechanical resonances above. It is thought that, since peak locking reduces the sensitivity of the cavity to length changes, these peaks are suppressed during such operations [12].

Results

HOM

Early tests revealed that the higher order cavity modes were easier to lock to than the fundamental. Figure 8 shows a selection of the transverse modes recorded.

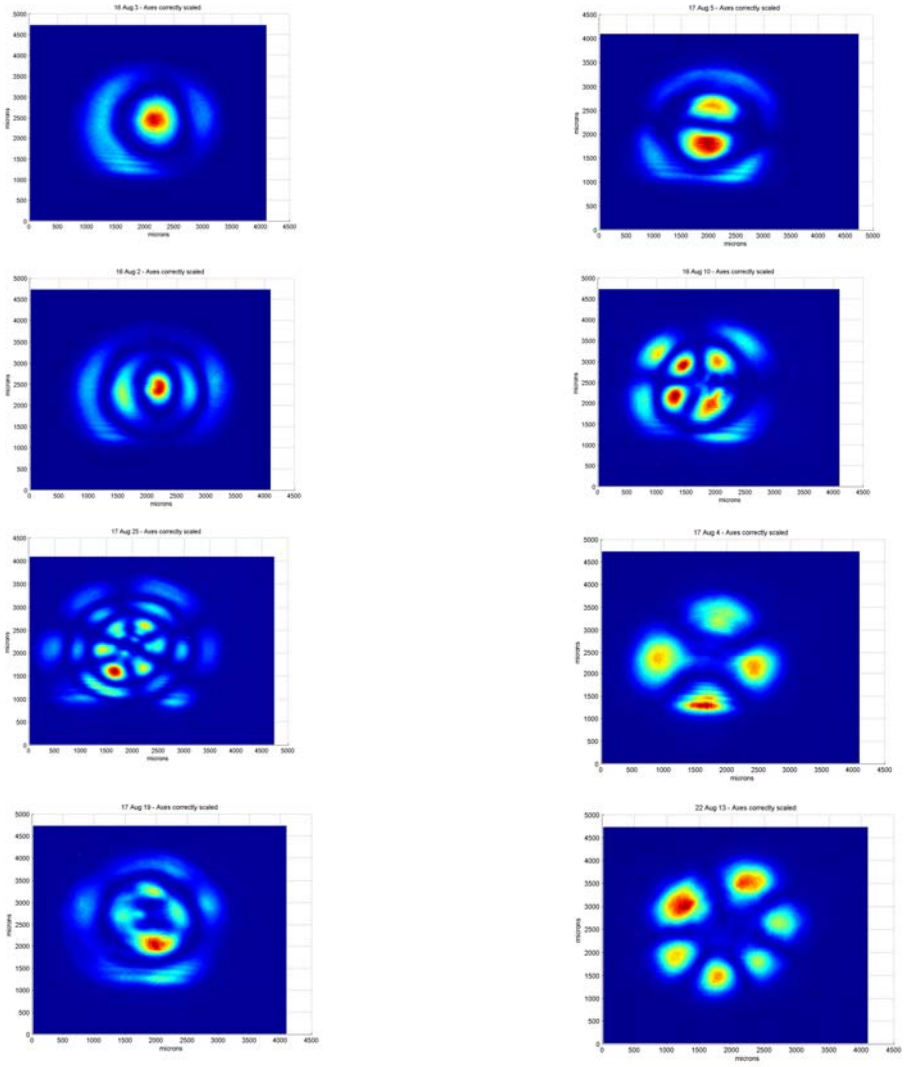

Figure 8. Higher order modes

Although these modes closely resemble the Laguerre-Gaussian and Hermite-Gaussian modes of a spherical mirror cavity they are quantitatively different. Figure 9 shows how attempts to fit a profile from our cavity to the TEM_{10} Laguerre and MH modes differ.

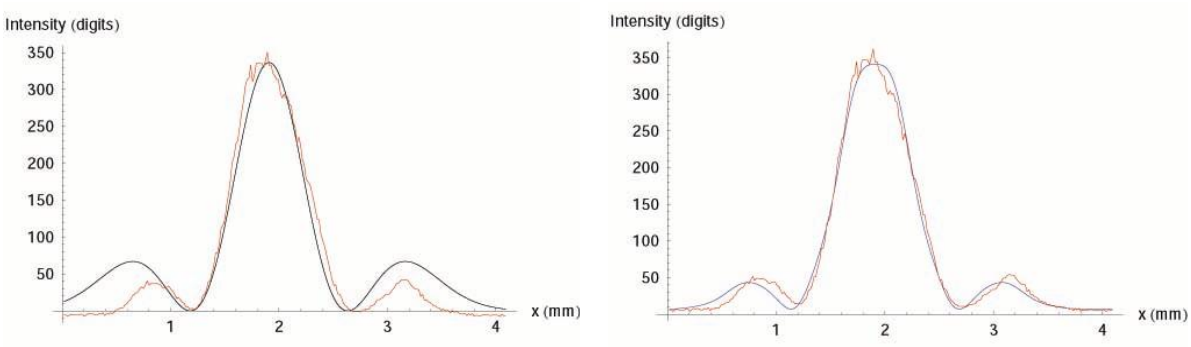

Figure 9. Fitting experimental profile with Laguerre-Gaussian (left) and MH (right) modes

We can conclude that these modes are definitely not the same as the Laguerre-Gaussian set and are in fact the MH eigenmodes.

One can also notice an asymmetry in the power distribution of these modes. This phenomenon has been a constant cause of consternation in the experiment. The same effect was also observed when a spherical EM was used, although it was generally less apparent due to the smaller Gaussian beam. Figure 10 shows a one and 2d non-linear fit of a HG_{10} performed using specially written MatLab code. One possible explanation of this phenomenon is the the effect of the deformation of the input and folding mirrors.

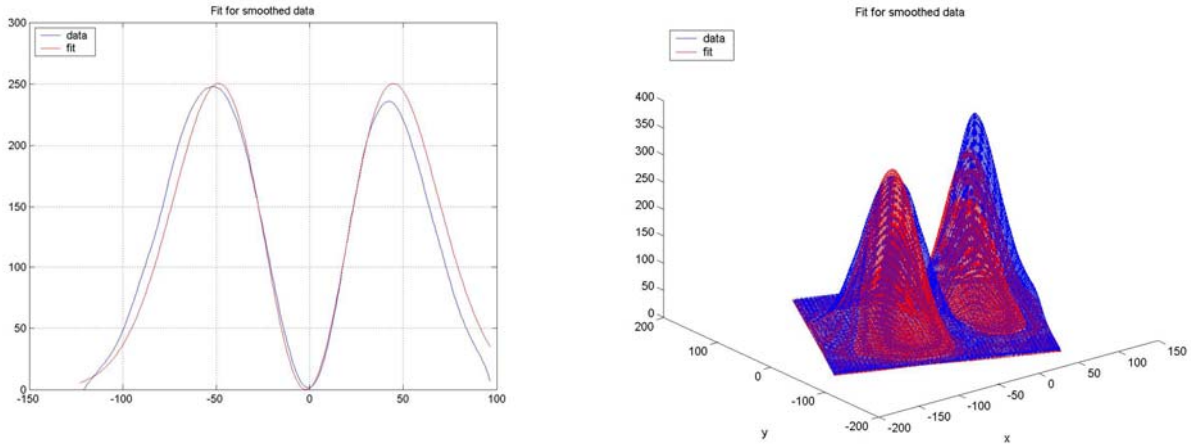

Figure 10. Asymmetry of HG_{10} with spherical end mirror. Data in blue, fits in red

The Fundamental

It was however more difficult to align to the fundamental. Figure 11 shows the best TEM_{00} achievable early in the project.

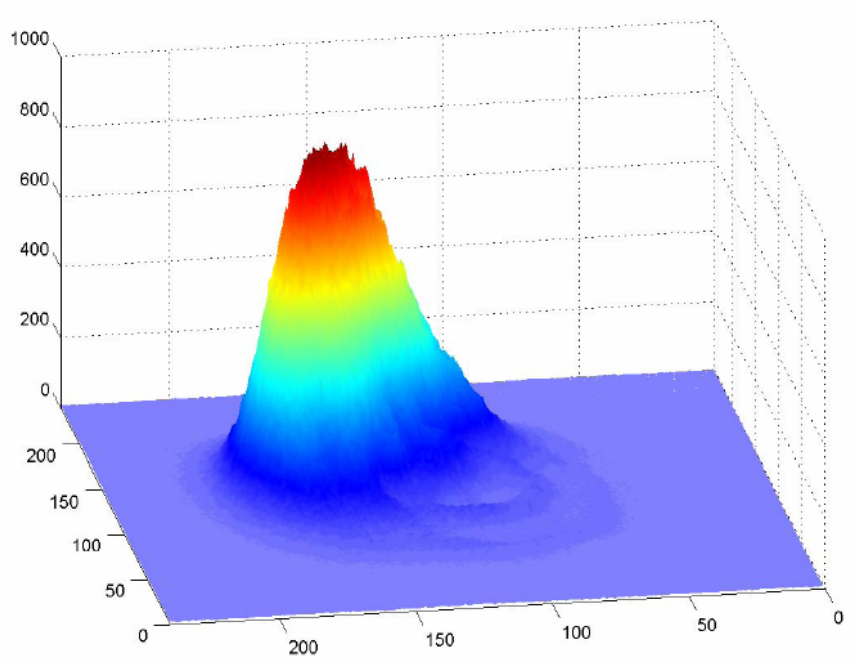

Figure 11. Best fundamental achievable in early summer

This field distribution can be explained as being caused by a tilt of one (or more) of the cavity optics (as seen in figure 6). Hence there is no definite procedure to produce the flat-topped beam from such a situation. Any attempt to drive the beam to a circular distribution resulted in the power 'snapping' to the same configuration on the opposite side of the mirror. Many attempts were made to re-align the cavity and input optics to alleviate this problem but all proved fruitless.

Improvements

Mode-matching

During initial tests with the MH EM the input beam mode-matching scheme was the same as that of the spherical mirror tests, producing an inefficient coupling.

Confronted with this situation a stop-gap attempt was made to improve the coupling of the input beam to the fundamental mode by deforming the input beam into a 'top-hat' shape (temporarily abandoning the goal of studying how efficiently a MH Fabry-Perot cavity 'cleans' a Gaussian input into MH modes). The two lens telescope of the spherical experiment was altered such that the first lens produced a highly divergent beam. The second lens was then used to focus only the central part of the large beam. This produced a spot size on the IM of the order of the correct size. This attempt to

inject a roughly flat-topped beam failed as no consideration of the phase of the beam was entered into. A more formal treatment was required.

In order to efficiently transmit energy from the Gaussian input beam to the cavity it is important to achieve the best approximation of a 'mode-match' between the two fields. The optimal radius of curvature at the input mirror is obviously $R = \infty$ to match the phase front to the flat optic. It was found that the optimal beam also had a waist size of $w_0^{MH} = 5.6\ mm$ [3]. The waist size of the gaussian input beam was measured to be $w_0^{IN} = 0.114\ mm$.[12] Hence our task was to increase the beam waist by a factor of 50 within a finite distance, also producing a plane wavefront on the input mirror.

This task was approached using the standard *ABCD* beam propogation matrices of [7]. We consider the system as shown in figure 12. The matrix of such a system is as given in (7).

$$\begin{bmatrix} A & B \\ C & D \end{bmatrix} = \begin{bmatrix} 1-\frac{d2}{f1}+d3\left(\frac{d2}{f1f2}-\frac{1}{f1}-\frac{1}{f2}\right) & d1+d2-\frac{d1d2}{f1}+d3\left(1-\frac{d1}{f1}-\frac{d1}{f2}-\frac{d2}{f2}+\frac{d1d2}{f1f2}\right) \\ \frac{d2}{f1f2}-\frac{1}{f1}-\frac{1}{f2} & 1-\frac{d1}{f1}-\frac{d1}{f2}-\frac{d2}{f2}+\frac{d1d2}{f1f2} \end{bmatrix} \quad (7)$$

We can now define the complex beam parameter at each waist (using the fact that $R=\infty$ at such a position)

$$q1 = \frac{j\pi (w_0^{IN})^2}{\lambda} \quad (8)$$

$$q1 = \frac{j\pi (w_0^{MH})^2}{\lambda} \quad (9)$$

We are now able to use equations (7), (8), (9) and (10) to form an equation, the real and imaginary parts of which are given in (11) and (12)

$$q2 = \frac{Aq1+B}{Cq1+D} \quad (10)$$

$$B = \frac{-C(\pi w_0^{IN} w_0^{MH})^2}{\lambda^2} \quad (11)$$

$$D = \frac{A(w_0^{IN})^2}{(w_0^{MH})^2} \quad (12)$$

We now have two equations and five variables, an insoluble problem. In order to produce a result the total length of the system *d1+d2+d3* was held constant at 3.1m (the maximum distance available in the laboratory). This allowed *d3* to be defined in terms of *d1* and *d2*. The focal lengths of the lenses were also fixed at standard values. Hence our only free variables are now *d1* and *d2*.

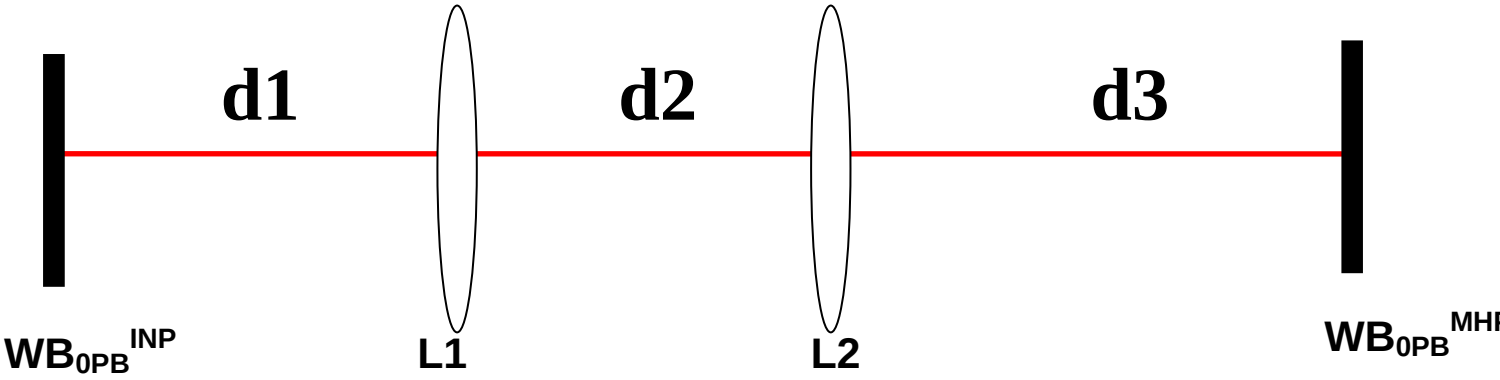

Figure 12. Diagram of mode matching problem

This method provides ideal mode-matching solutions provided that the calculated values of *d1* and *d2* are implemented with high precision. To quantify the 'goodness of match' the following quantity, which we aim to minimise, was introduced

$$Q = \frac{1}{2}\left(\frac{w^{mirror} - w_0^{MH}}{w_0^{MH}}\right)^2 + \frac{1}{2}\left(\frac{Pos_{w_0^{MH}} - (d1 + d2 + d3)}{2z_R}\right)^2 \quad (13)$$

Q considers the discrepancy between the waist on the input mirror w^{mirror} and the ideal waist and also the position of the ideal waist with respect to the input mirror.

Various standard lens combinations were found to produce solutions. However, it was found that small perturbations away from the fiducial alignment caused the Q of the system to balloon - this type of solution is unstable. We can see this studying figure 13. The x axis (in mm) shows that for perfect values of *d1* and *d3* any small perturbation, *delF*, of *d2* results in a high Q value.

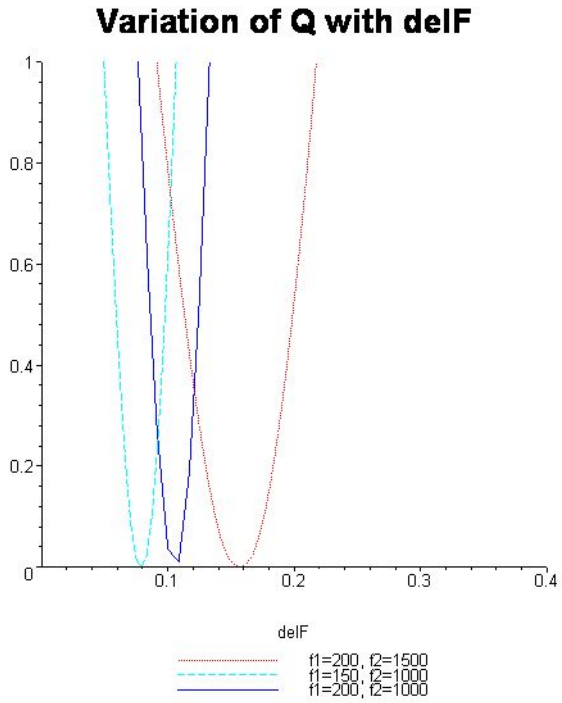

Figure 13. Two-lens mode matching solutions proved unstable

It was decided that this solution required an accuracy which would be taxing to achieve. We then sought a simpler, more stable solution.

If we apply an analogous procedure to a one-lens mode matching telescope, even if it may lead to a poorer mode matching, it is trivial to show that any lens with $f>f_0=(\pi w_0^{IN} w_0^{MH})/\lambda$ can be used to mode-match the input beam to the cavity as long as the distance from w_0^{IN} to the lens, *d1*, and the distance from the lens to w_0^{IN}, *d2*, satisfy (14),(15) (choosing either + or - in both equations). For further detail see, for example, [7].

$$d1 = f \pm \frac{w_0^{IN}}{w_0^{MH}} \sqrt{f^2 - f_0^2} \quad (14)$$

$$d2 = f \pm \frac{w_0^{MH}}{w_0^{IN}} \sqrt{f^2 - f_0^2} \quad (15)$$

These equations dictate that a one-lens system giving our required magnification be ~ 40m long. However if we permit non-perfect matching we are able to produce a stable, practically beneficial, solution. Hence a one lens telescope with *d1*=2033mm, *d2*=830mm and *f*=2033mm was selected. Although not optimal this configuration gives a *Q* value of 0.002 [12] and has sufficient stability to be easily implemented.

Warped mirrors

Implementation of the new mode-matching scheme made a small improvements to the observed profile but the fundamental remained elusive.

LMA were keen to stress the importance of using thick, rigid substrates to make the MH mirrors. Hence it was decided to investigate the, thinner, flat, folding and input mirrors. Interferometric mapping of the mirror surfaces revealed substantial deviations from flat, see figure 14.

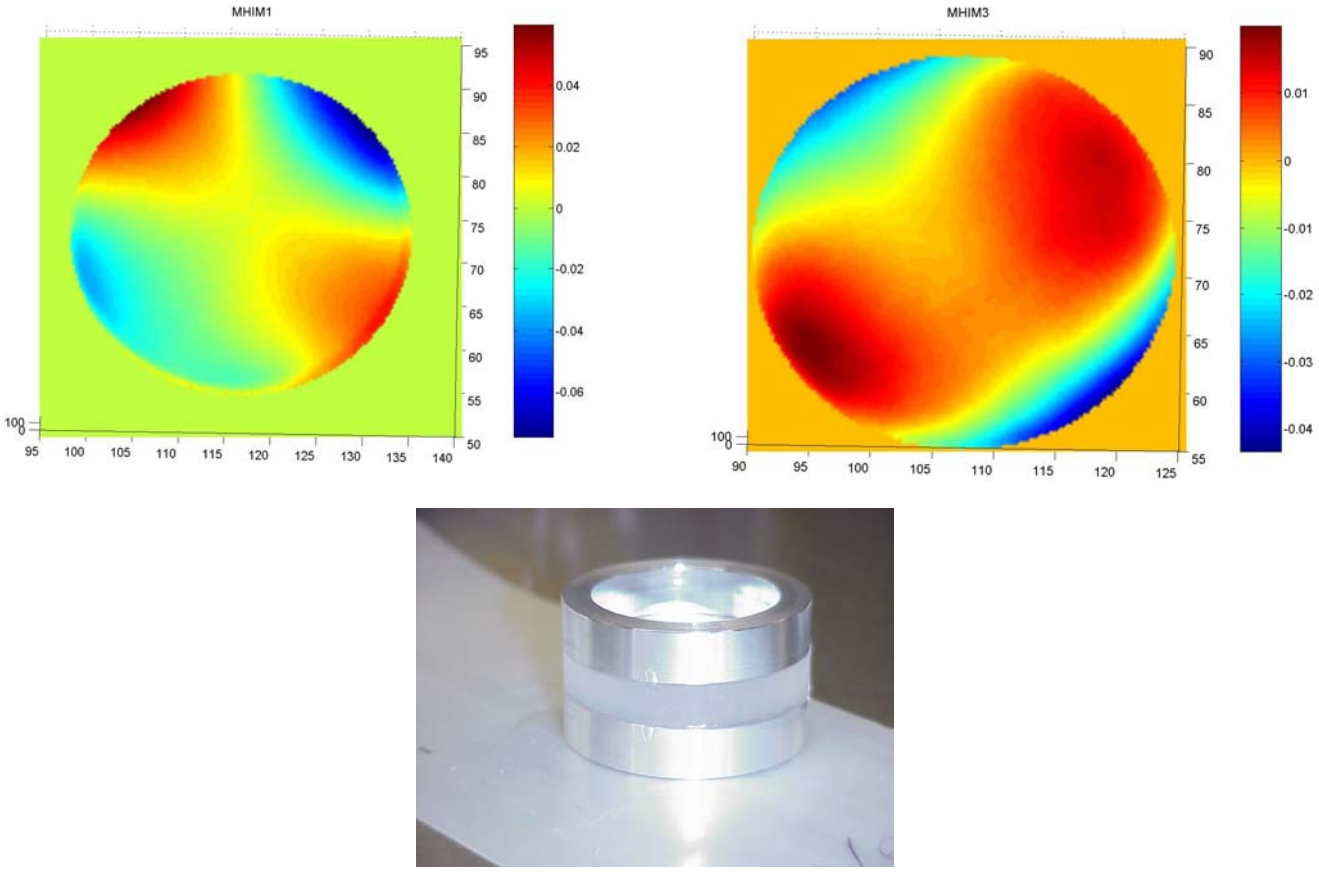

Figure 14. Warped and fixed mirrors. Colourbar units are microns

The amplitude of deviation from flat was found to be ~ 60nm across the mirror surface. This level of accuracy (λ/18) may be sufficient for most applications using Gaussian beams (they examine smaller fractions of the mirror's surface) but a deviation of 60nm represents a feature with a size which is 300\% of the size of the MH mirror's central bump.

No relevant deformation from the manufactured profile was observed in the MH mirror. This leads us to believe that the deformation can be attributed to the thinner mirror substrates. The MH substrate it three times thicker than that of the two flat mirrors. Hence, to first approximation the flat mirrors are 27 times more flexible. The origin of this deformation seems to have been localised stress applied by the three PZTs on one face of the mirror and spring loaded pins on the other. This hypothesis is supported by two observations. The first is that the IM exhibited a larger deformation than the FM, possibly due to more frequent handling and higher stresses on the micrometric alignment screws. Secondly, the observed cavity modes worsened with each alignment. When adjusting the mirror orientation, the micrometric screws were invariably tightened (because of stiction) increasing the stress on the mirrors.

To ameliorate this problem it was decided to reinforce the mirrors with two aluminium rings (see figure 14). These rings spread the efforts and replaced a spacer gasket with double the thickness of one ring thus maintaining the overall length of the system (happily the mechanics had been designed for thick and rigid mirrors everywhere). This endeavour reduced the size of the deformation by a factor of about 3. Additionally, the gradient over the central portion of the mirror- where the beam is ideally incident- was even more significantly reduced.

Atmospheric isolation

Post mirror strengthening considerable improvements were observed. To take advantage of these improvements better ‘in lock’ stability was required as this would allow us to fine tune the PZT alignment without jumping to a HOM. To this end the two not-yet-implemented barrel and end-plate heat shields were installed thus mitigating the impact of air density variations within the lab, see figure 15.

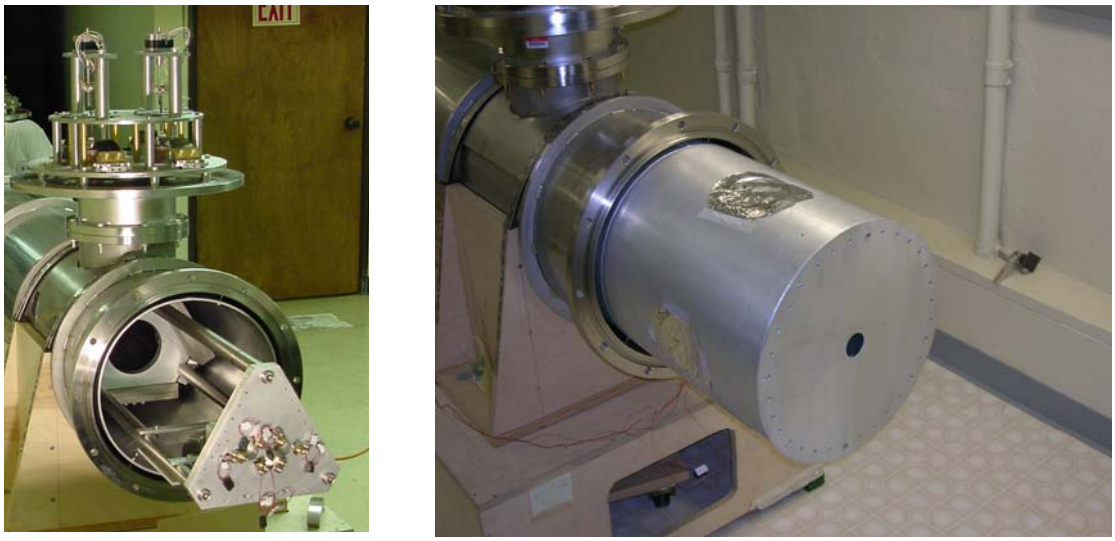

Figure 15. Cavity with and without heat shield end plate

These plates were designed assuming that the cavity would hang centrally in the vacuum tank. This was not the case and larger apertures had to be machined to avoid diffraction induced problems. I am grateful to Chiara Vanni for her assistance in this area.

The key step

The above aside, the principal change that allowed us to observe the mesa beam for the first time was a switch in experimental technique. Instead of aligning the cavity and input optics using transverse field profiles as a reference we switched to using the mode spectrum. The cavity was subsequently aligned so that it favoured the fundamental mesa beam above all others. This not only improved the profile but also our ability to lock to it. Figure 16 shows what difference this change made to the spectrum.

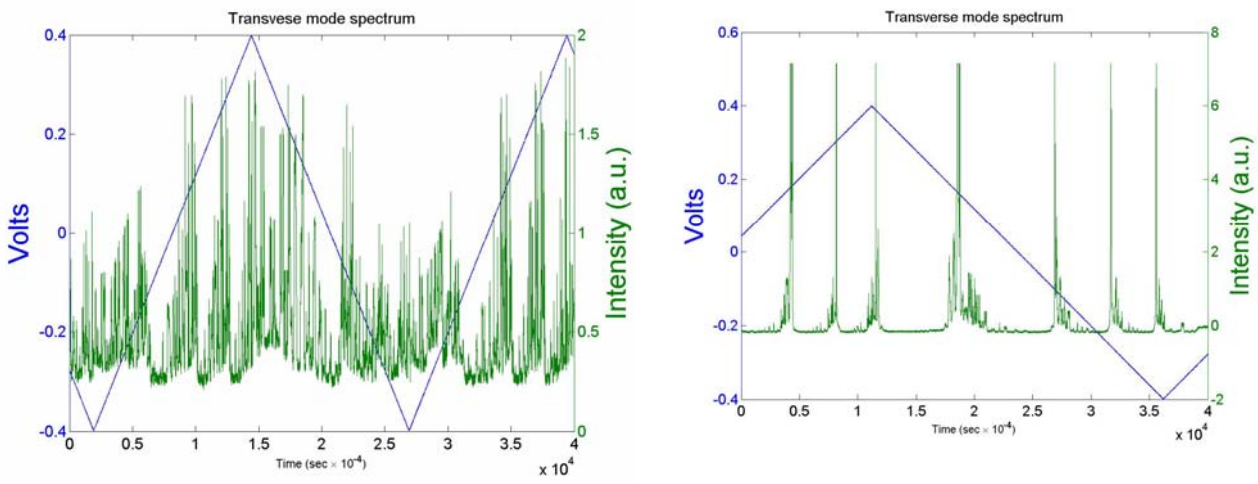

Figure 16. Improvement in transverse mode spectrum. Left: initially alignment was made with the goal of producing a good beam profile on CCD1. Right: Subsequently alignment was approached with the goal of producing the best transverse mode spectrum.

Notice that as well as having a accentuated fundamental the overall intensity is much greater.

Finally on the 22nd of August the first mesa beam was observed. Figure 17 shows the improving alignment and figure 18 shows the mesa profile achieved.

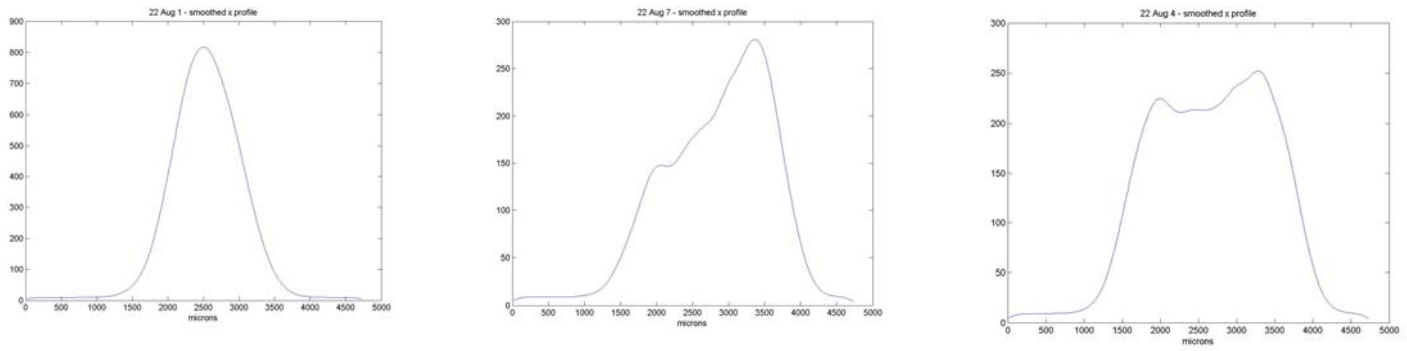

Figure 17. Aligning the first mesa beam

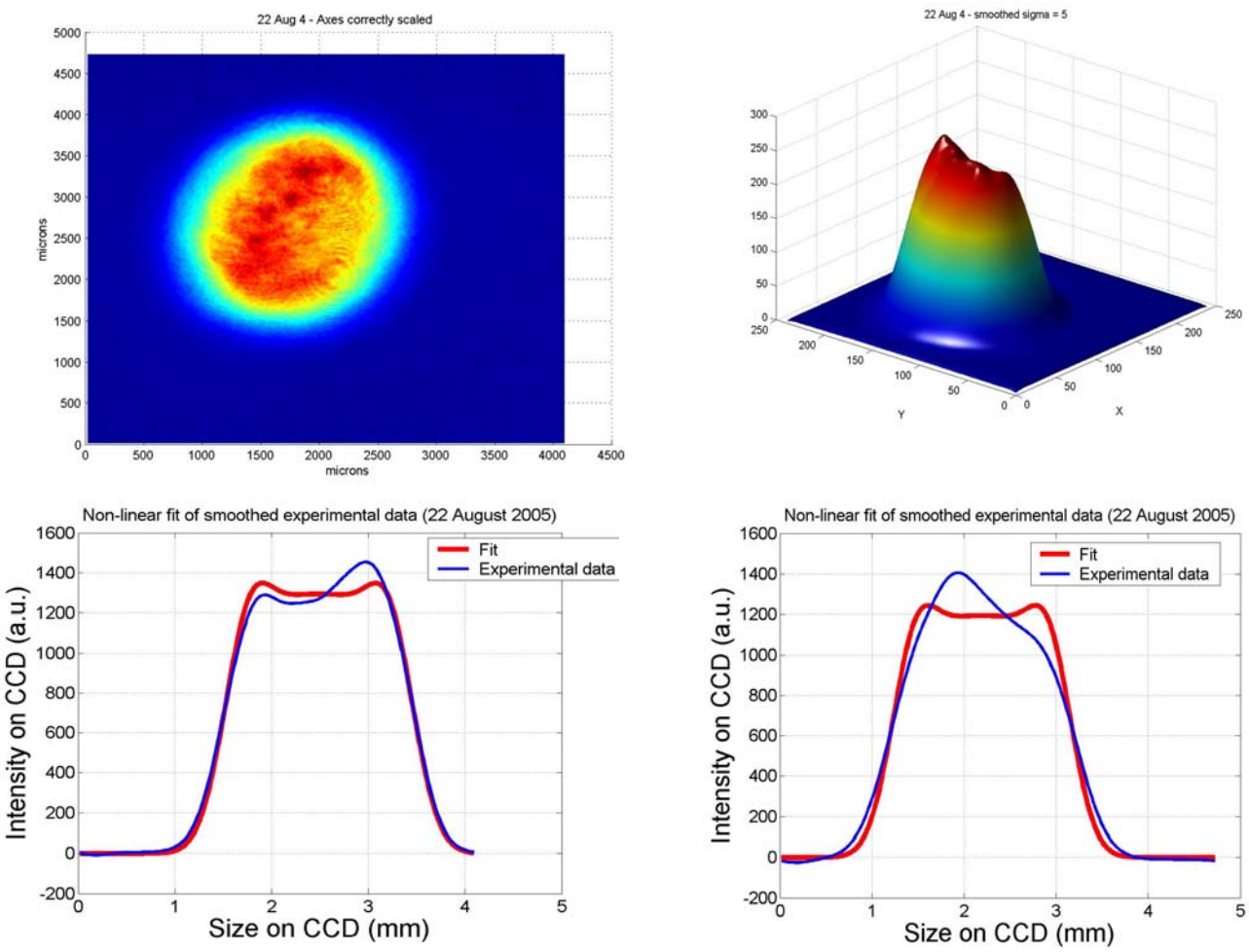

Figure 18. First mesa beam

The non-linear fits shown figure 18 yielded a value for the size of the minimal Gaussian used to model this beam and hence a value for the size of the beam *on the CCD*. To compare the captured beam to theoretical predictions from FFT code simulations it was necessary to convert the beam size on the CCD to the beam size on the FM.

The beam propagation through the readout optics was modelled as a geometric problem using (16), [8].

$$\begin{bmatrix} \rho_2 \\ \theta_2 \end{bmatrix} = \begin{bmatrix} A & B \\ C & D \end{bmatrix} \begin{bmatrix} \rho_1 \\ \theta_1 \end{bmatrix} \quad (16)$$

where the *ABCD* matrix is that of the two lens system above (see (7)). Figure 19 shows the readout optics. Knowing ρ_2 and assuming $\theta_1 = 0$ one is able to find the size of the beam on the folding mirror of the cavity.

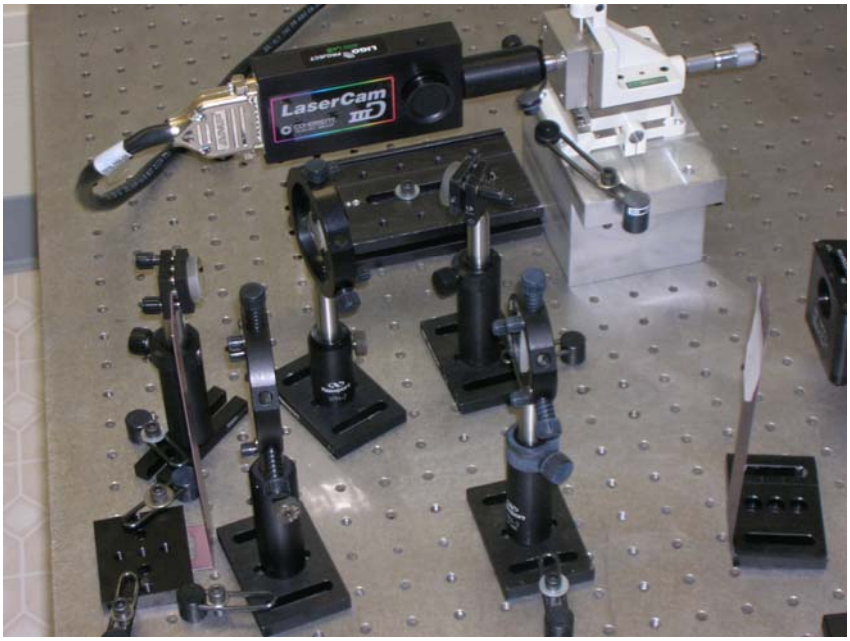

Figure 19. Readout optics,cf, figure 5

The results were as follows: Beam size on FM from experiment - 7.60 ±1.19mm; beam size from theoretical considerations - 6.68mm [12]. For the current best mesa beam see Appendix A.

The results agree within experimental error the main source of which lies in the measurement of the distances between the optics in figure 19.

Tilt

Above we have shown that it is possible to produce predominantly flat-topped beam profiles even with imperfect mirrors. This technology is being proposed as a possible scheme for AdvLIGO and hence we are greatly interested in not only the generation but also the controllability of the beam. The first inroads into this investigation were made this Summer and will continue in the future.

It was decided to first investigate the susceptibility of the mesa field to tilts of the MH mirror. Many theoretical investigations have been carried out in this area [9, 10, 2]. The alignment tolerances for a MH mirror cavity are thought to be ~3 times more stringent than those of the fiducial (gaussian beam) design. We aim to provide experimental data allowing the confirmation or rejection of this hypothesis.

Calibration

To achieve this ambitious goal an accurate calibration of the PZTs was required. This was achieved through determining the input voltage required to sweep the cavity through a known number of free spectral ranges (FSRs).

Various triangular swept-sine waves of different amplitudes and frequencies were applied to the input of the PZT driver circuit.

The transverse mode spectra were then recorded using a dedicated *LabView* virtual instrument. Figure 20 shows a section of recorded data. Knowing that the distance between corresponding peaks of different FSR corresponds to λ/2=532nm we are able to obtain a value of PZT displacement for a unitary voltage input.

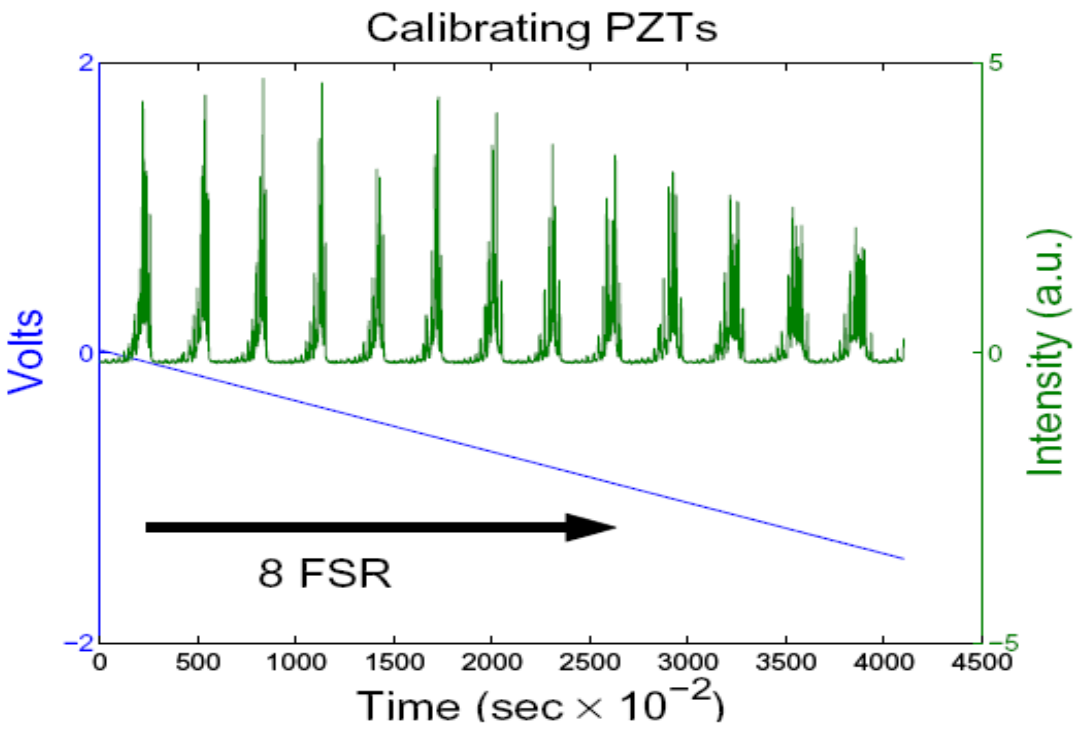

Figure 20. Calibrating the PZT actuators

Although the spectrum changes its form over the course of the voltage ramp (probably due to a differential in the gains of the PZTs) it is nevertheless believed that the final value is sound. The extrapolated experimental open loop travel for 0-100V applied directly to the PZTs showed good agreement with the manufacturer's specification:

$$T^{100}_{experimental} = 15.66 \pm 0.16 \mu m$$

$$T^{100}_{manufacturer} = 15 \mu m$$

Experiment

Initial experiments were carried out adjusting the mirror's angular position using the 5K pots on the PZT driver. These variable resistors display their relative impedance in arbitrary units on digital displays. Reviewing the data obtained it was thought that these devices lacked the resolution required for such an experiment. We then switched to the use of a d.c. power supply (HP E3610A) connected to the PZT driver input. This improved matters. This supply has a digital display, limiting one to discrete increments of voltage. To further reduce the minimum control voltage step on the piezos a voltage divider could be incorporated into the system.

During alignment and locking to the fundamental mode a constant voltage from the supply was applied to one PZT channel. Starting with a non-zero voltage allows one to both increase and reduce the voltage thus tilting the mirror through positive and negative angles relative to the initial position. This initial alignment was carried out using the output of the high resolution CCD2 (see figure 5) producing better profiles than previously. The d.c. voltage applied was then adjusted using the smallest intervals allowed by the supply. At each stage a profile was captured.

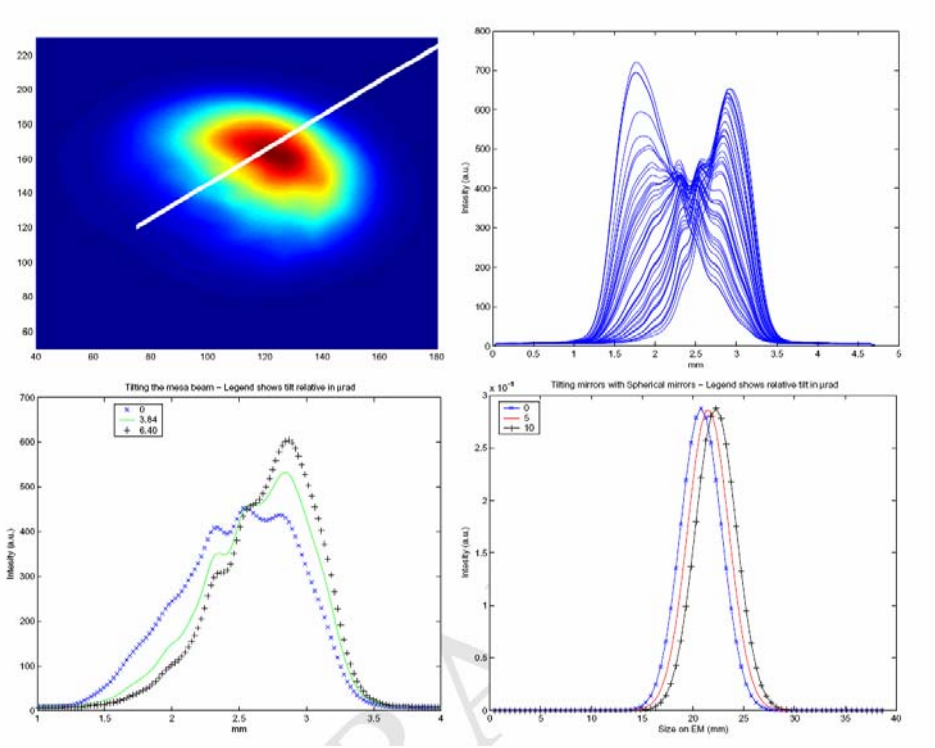

Figure 21. Quantifying tilt sensitivity. Clockwise from top-left: Density plot showing section through which profiles were taken; all profiles taken during the second data run; selected profiles; simulated profiles detailing the effect of tilts on a spherical mirror cavity [11]

Analysis

The first results from this experiment revealed that the system suffered from backlash or hysteresis (characteristic of piezos moving over small distances). This was noted and during analysis only data taken with the PZTs moving in the same direction were directly compared. Initial results from this experiment are shown in figure 21.

From the last two images one can see the disparity of behaviour between the spherical and MH mirror cases. A tilt of a spherical mirror results only in a translation of the optical axis with little effect on the power distribution. One may also observe the asymmetry in the effect of equal tilts. This may be due to the tilt of the central ‘bump’ of the current MH mirror. This probably derives from the fact that the ideal alignment already has a compensating tilt of ~1µrad, hence tilts in opposite directions can have a different effect.

We can compare this data to FFT simulation [11]. Figure 22 shows a comparison between theoretical tilts of a MH cavity (with perfectly flat input mirror and the real map of the experimental MH mirror (5008)) and experimental data.

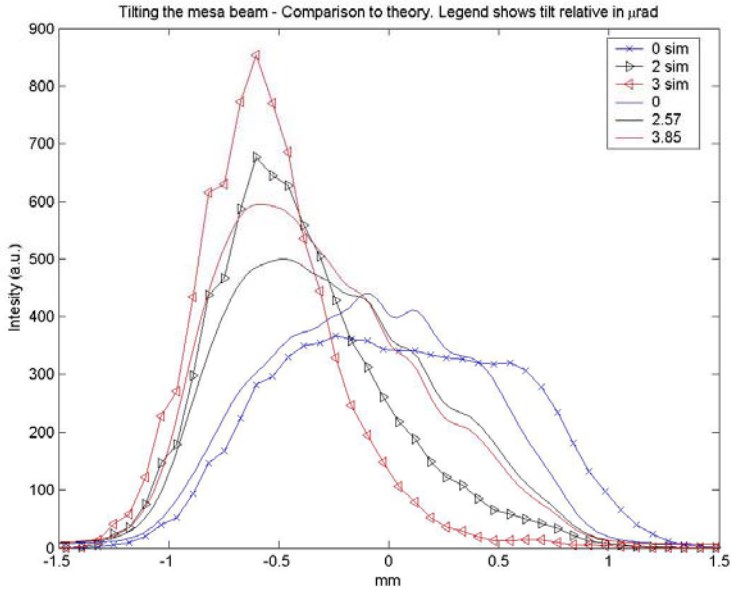

Figure 22. Tilt sensitivity of the MH mirror cavity

Qualitatively there is strong agreement between the general trends of both theoretical and experimental data. Tilts cause the power to skew to one side of the mirror and become strongly peaked - thus destroying the benefits of a mesa beam. Quantatively we see that experimental tilts have a smaller affect on the profile by a factor of ~2.

Several caveats must be considered when examining this data. This is only the second data set and experimental technique may not yet be honed; the resolution of the power supply used to tilt the mirrors is limited (error in angular position is ±0.6μrad); there is opinion that the quasi-monolithic mirror mounts may be suffering from stiction so that mirror tilt is not directly proportional to input voltage; the simulations also consider the optimal alignment which may not be used in the lab; problems of temporal stability are also being investigated, see figure 23. In certain instances long-term drifts produce the same effect as a mirror tilt. For example, the results of figure 23 could cause one to over or underestimate the effect of a tilt in the orthogonal direction. This problem may be cured by switching to vacuum operation.

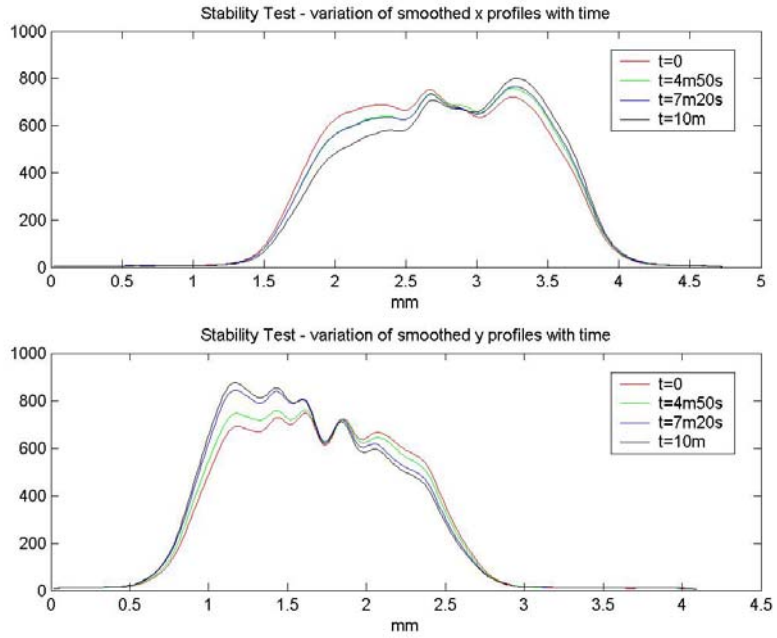

Figure 23. Temporal stability of the mesa beam

Further work

Much progress has been made with the MH interferometer this Summer. We have produced good fundamental modes with imperfect optics and begun the quantitative characterisation of the beam's properties. Still, much work remains - the assessment of tilt sensitivity is still in its infancy and only one of three MH mirrors has been investigated. Studying the other two may allow us to quantify the beam profile sensitivity to mirror imperfections and to define manufacturing tolerances for LIGO sized optics.

All of this work will be expedited by the introduction of new, thicker and flatter, input and folding mirrors along with complementary mounts. The current mounts not only contributed to mirror deformation but were also toilsome to use. The copper springs often lack the restorative force to return the mirrors when micrometric screws were unwound, they also hindered mirror dithering in the latter stages of this investigation. The new mounts will incorporate appropriate measures to ensure mirror rigidity. Other improvements may include the implementation of Pound-Drever-Hall reflection locking and auto-alignment systems.

The future

At Caltech, probable developments involve the design and application of a new type of MH mirrors to the current cavity. These mirrors will be constructed starting from a spherical substrate and will yield a nearly concentric cavity. This configuration is

predicted to be more stable against radiation pressure effects whilst still offering the same benefits as the current scheme. Perhaps further afield may be the construction of a MH Thermal Noise interferometer to directly measure the predicted improvements. This experiment would require larger scale facilities such as TAMA or AIGO.

Appendices

Current best fundamental

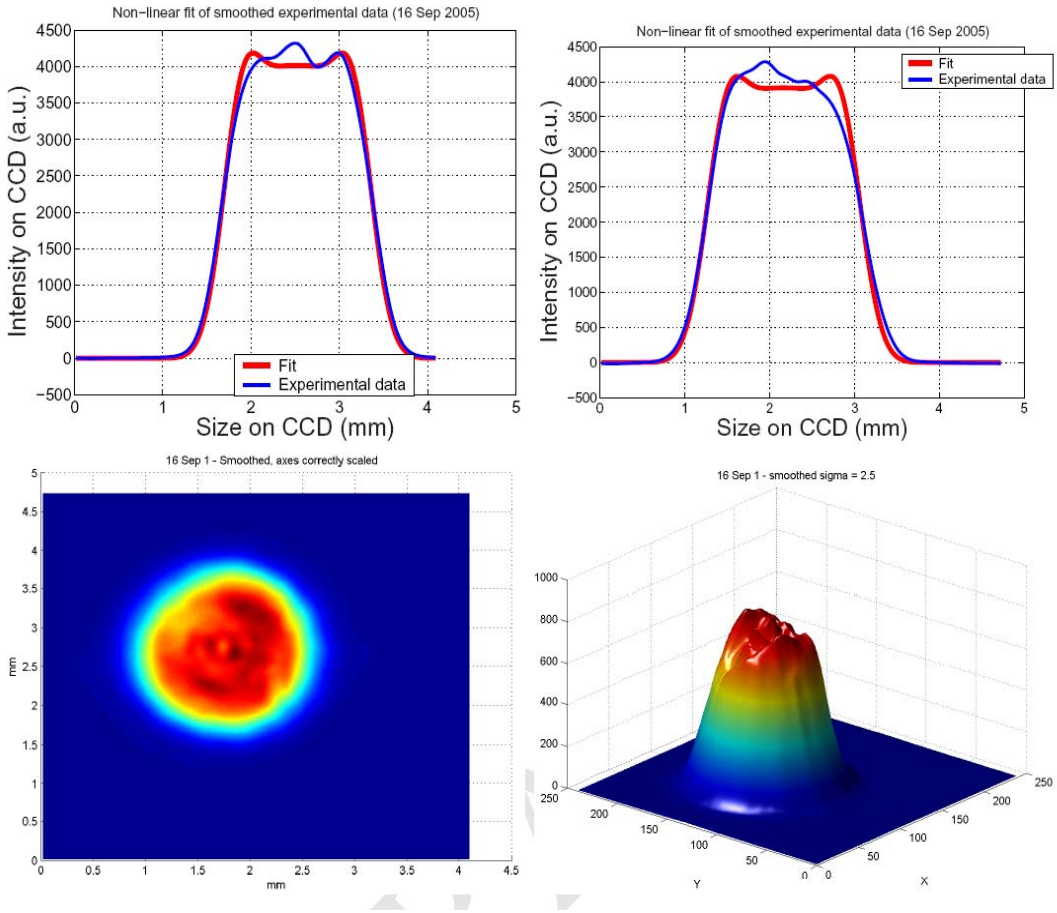

Figure 24. Current best fundamental

$w_{experimental} = 6.84 \pm 1.10 mm$

$w_{theory} = 6.68 mm$

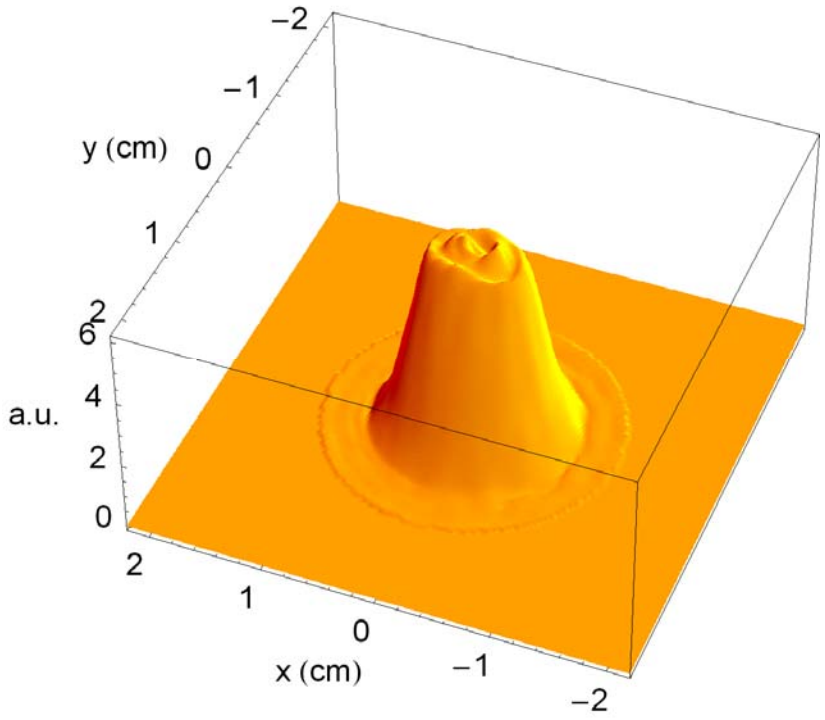

Figure 25. FFT simulation of best possible fundamental using our current MH mirror and perfect input and folding mirrors

Acknowledgements

I would firstly like to thank my mentor Riccardo DeSalvo for being the indefatigable driving force behind the project, ever present with words of encouragement in times of despondency. Although Dr.DeSalvo was nominally my mentor acknowledgement must be given to the contribution to this work made by Phil Willems. Phil was very much the ideas man who often sent me back to the lab with numerous new avenues to explore. Special thanks is also given to Marco Giacinto Tarallo for all his help and understanding. He fielded more than his fair share of naive and/or stupid questions. Juri Agresti also merits mention for the help he unerringly offered over the fifteen weeks of my stay. Other people in the LIGO lab who helped with various aspects of my work are Mike Smith (mode-matching), GariLynn Billingsley (mirror mapping), Chiara Vanni (mechanical set-up, an area in which she is expert). Alex and Dan also made the time spent in the lab more enjoyable.

Many people made my time at Caltech more than just a research experience. I would like to mention Dámaris, Jeff, Jim, Marleen, Jason, Ross, Ryan, Thomas, Alberto and everyone from lunch and merenda. Additionally I am grateful to everyone who took the time to translate for me. Thanks to these generous souls my Italian vocabulary (most of which is unsuitable for polite conversation) now extends into double figures.

I also acknowledge the help given to me with my application by Jim Hough and Harry Ward from Glasgow.

The LIGO Observatories were constructed by the California Institute of Technology and the Massachusetts Institute of Technology with funding from the National Science Foundation under Cooperative Agreement PHY-9210038. The LIGO Laboratory operates under Cooperative Agreement PHY-0107417.

Any opinions, findings, and conclusions or recommendations expressed in this material are those of the author and do not necessarily reflect the views of the National Science Foundation.

Bibliography

[1] Braginsky, Gorodetsky and Vyatchanin, 1999, *Phys Lett.A Vol 264*

[2] D'Ambrosio E *et al* Classical and Quantum Gravity **21** S867-S873

[3] D'Ambrosio E 2003 "Nonspherical mirrors to reduce thermoelastic noise in advanced gravitational wave interferometers" *Phys. Rev. D,* **67**, 102004

[4] D'Ambrosio E *et al* 2004 "Reducing Thermoelastic Noise in Gravitational-Wave Interferometers by Flattening the Light Beams" *Phys. Rev. D* in preparation

[5] Simoni B 2004 "Design and Construction of a Fabry-Perot Cavity for Gaussian and Non-Gaussian Beam Testing. Preliminary Test with Gaussian Beam" Tesi di Laurea Specialistica, Università di Pisa LIGO-P040037-00-R

[6] Agresti J *et al* 2005 "Design and Construction of a Flat Top beam interferometer and initial tests" Amalidi 6 Conference Proceedings

[7] Kogelnik, Li, 1966, *Applied Optics Vol. 5 No. 10*

[8] Fowles G R, 1989, *Introduction to Modern Optics*

[9] Savov P, Vyatchanin S 2004 "Estimate of Tilt Instability ofMesa-Beam and Gaussian-Beam Modes for Advanced LIGO" *ArXiv General Relativity and Quantum Cosmology e-prints* 0409084

[10] O'Shaughnessy R, Strigin S, Vyatchanin S 2004 "Theimplications of Mexican-hat mirrors: calculations of thermoelastic noise and interferometer sensitivity to perturbation for the Mexican-hat-mirror proposal for advanced LIGO" *Phys. Rev D* in preparation

[11] Agrest J 2005 Private communication

[12] Tarallo M 2005 "Experimental study of a non-gaussian Fabry-Perot resonator to depress mirror thermal noise for gravitational waves detectors" Tesi di Laurea Specialistica, Università di Pisa LIGO-P050032-00-R